ELSEVIER

Polymer 41 (2000) 4849–4862

polymer

Fish oil thermosetting polymers: creep and recovery behavior

F. Li[a,b], R.C. Larock[b], J.U. Otaigbe[a,c,*]

[a]*Department of Materials Science and Engineering, Iowa State University, Ames, IA 50011, USA*
[b]*Department of Chemistry, Iowa State University, Ames, IA 50011, USA*
[c]*Department of Chemical Engineering, Iowa State University, Ames, IA 50011, USA*

Received 15 June 1999; received in revised form 13 September 1999; accepted 14 September 1999

Abstract

We report creep and recovery behavior of novel polymers prepared by the cationic copolymerization of fish oil (FO) and conjugated fish oil (CFO) with a number of comonomers using boron trifluoride diethyl etherate as the initiator. The experimental results are compared with classical models of linear viscoelasticity and structural effects on the creep behavior are examined. The models successfully predict the creep behavior in the static loading range of 0.03–0.07 MPa, together with a retardation time distribution function, suggesting that the materials are linearly viscoelastic under the test conditions. Deviations between experimental results and theoretical predictions are explained in terms of structural effects being controlled by the nature and conjugation of the double bonds in the fish oils, as well as the interactions of the unreacted oils with the crosslinked network structure of the polymers. At high temperatures, the CFO and divinylbenzene copolymers show better creep resistance and higher strain recovery than that of the FO polymers. These results together with those obtained from dynamic mechanical analysis indicate that the polymers may be useful in applications where commercial viscous fish oil systems are not usable.

Keywords: Creep and recovery; Fish oil; Thermosetting polymers

1. Introduction

Due to the potential limitation of petroleum resources as well as increasingly stringent environmental concerns [1,2], polymers derived from renewable natural resources have recently become one of the most important subjects for research and development. In contrast to polymers derived from petroleum resources, these polymers are inexpensive, environmentally friendly and can be made to biodegrade safely during use [3].

Fish oil, a by-product of fish meal, is readily available. Typically, fish oil has a triglyceride structure with a high degree of unsaturation [4-6]. The commercial Norway fish oil (FO) used in this study is a mixture of ω-3 fatty acid ethyl esters [7,8]. Because of the multitude of carbon–carbon double bonds, these molecules are suitable for cationic polymerization [9,10]. However, in the past the cationic polymerization of fish oil has resulted in polymers that were always viscous fluids with limited uses [5]. The reactivity of fish oil can be significantly improved by conjugating its double bonds [11] and the resulting polymers are generally soft, weak rubbers. In the present study, hard plastics have been obtained when the fish oil is copolymerized with certain comonomers, such as divinylbenzene (DVB), norbornadiene (NBD) or dicyclopentadiene (DCP) [8]. These polymers are thermosetting and may be an alternative source of polymers to the petroleum-based plastics in many applications, such as structural materials. In addition, the present plastics are expected to be good binders for fiber-reinforced polymer composites [12]. In the targeted applications for the fish oil plastics, the materials are subjected to a variety of stress and strain histories and their creep resistance behavior is of prime concern. The creep performance is not only one of the main criteria to assess the long-term performance of the materials in practical applications, but it is also of major importance in determining and explaining the molecular origins of viscoelasticity in these materials [13]. In previous papers, we reported our progress in understanding the relationships of the synthesis, structure and thermophysical properties [8,14]. In this paper, we report our results on the creep performance and the subsequent strain recovery behavior of these polymers. An interesting supermolecular structure is used to explain the observed creep behavior of the polymers. The structure and creep deformation

* Corresponding author. Department of Materials Science and Engineering, Iowa State University, Ames, IA 50011, USA. Tel.: +1-515-294-9678; fax: +1-515-294-5444.
E-mail address: otaigbe@iastate.edu (J.U. Otaigbe).

0032-3861/00/$ - see front matter
PII: S0032-3861(99)00702-8

Table 1
Compositions of the native and conjugated fish oil polymers

Samples		Fish oil	DVB	NBD	DCP	Initiator
FO-DVB-38	mol%	37.7 FO	54.6			7.7
	wt%	62.5 FO	32.7			4.8
FO-DVB-NBD-38	mol%	37.7 FO	32.0	22.6		7.7
	wt%	65.0 FO	20.0	10.0		5.0
FO-DVB-DCP-38	mol%	37.7 FO	36.6		18.0	7.7
	wt%	62.4 FO	21.9		10.9	4.8
CFO-DVB-38	mol%	37.7 CFO	54.6			7.7
	wt%	62.5 CFO	32.7			4.8
CFO-DVB-NBD-38	mol%	37.7 CFO	32.0	22.6		7.7
	wt%	65.0 CFO	20.0	10.0		5.0
CFO-DVB-DCP-38	mol%	37.7 CFO	36.6		18.0	7.7
	wt%	62.4 CFO	21.9		10.9	4.8

relationship, if it is generally applicable to all polymers derived from food grade oils, is encouraging in terms of predicting creep rates from the characteristics of cationic copolymerization of these oils which in turn are connected to intramolecular and intermolecular features.

2. Experimental

2.1. Materials

Native fish oil (FO) (Norwegian Pronova EPAX 5500 EE Lot no. 60301) supplied by Pronova Biocare, Bergen, Norway was used in this study. Its average molecular weight is calculated to be 360 g/ml based on its composition [7]. Conjugated fish oil (CFO) was prepared from the above native fish oil in our lab using Wilkinson's catalyst [$RhCl(PPh_3)_3$]. The procedure for conjugation of the FO is described elsewhere [15]. The degree of conjugation was calculated to be about 90%. Conjugation does not change the molecular weight of the fish oil, but converts less reactive isolated double bonds into more reactive conjugated double bonds. The comonomers (DVB, NBD and DCP) were analytical reagents purchased from Aldrich Company and used as received. The boron trifluoride diethyl etherate ($BF_3{\cdot}OEt_2$, distilled grade) initiator (Aldrich) was used without further purification.

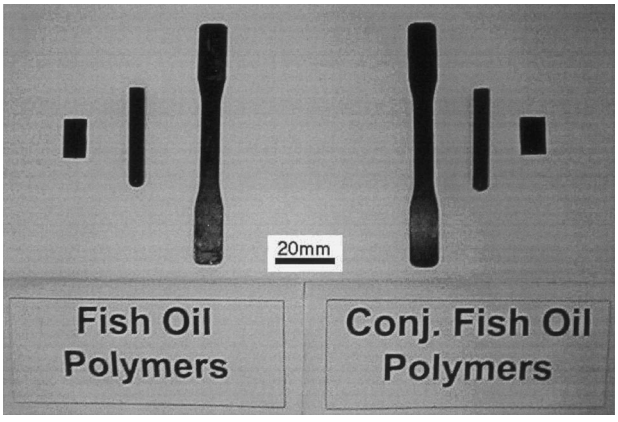

Fig. 1. Photograph of the native and conjugated fish oil polymers.

2.2. Cationic copolymerization

The desired amounts of comonomers and the initiator were added to the FO or CFO. The reaction mixture was stirred and sealed under air atmosphere. The sealed reaction mixture was then heated for a given time at appropriate temperatures. The relative compositions of the reactants used in this study are listed in Table 1. The nomenclature adopted in this paper for the samples is as follows: FO and CFO represent native fish oil and conjugated fish oil, respectively; DVB, NBD and DCP denote divinylbenzene, norbornadiene and dicyclopentadiene comonomers, respectively. For example, CFO-DVB-DCP-38 corresponds to a sample prepared from conjugated fish oil with divinylbenzene and dicyclopentadiene comonomers; the mole percent of fish oil is 38%. The ratio of DVB to DCP or NBD was maintained at 2 (wt/wt). The amount of initiator used for the preparation of all polymers was approximately 7.7 mol%. Fig. 1 shows photograph of the resulting FO and CFO polymers. Typically, these polymers are rigid, and have a dark-brown glossy color and a special odor. They can be made into various shapes using appropriate matched moulds. Table 2 summarizes the structure and physical properties of the polymers. The table shows that these polymer materials have densities of approximately 1000 kg/m^3, which appears to be independent of their compositions.

2.3. Soxhlet extraction by methylene chloride

A 2-g sample was extracted with 100 ml of refluxing solvent (methylene chloride) using Soxhlet extraction in air for 24 h. After extraction, the resulting solution was concentrated by rotary evaporation and subsequent vacuum drying. The soluble substances were isolated for further characterization. The insoluble solid was dried under vacuum for several hours before weighing.

2.4. Measurements

Dynamic mechanical analysis (DMA) data were obtained using a Perkin–Elmer dynamic mechanical analyzer Pyris DMA-7 in a three-point bending mode. Thin rectangular specimens of 1 mm thickness and 2.5 mm depth were used, and the span to depth ratio was around 5.0. The experiments were performed at a heating rate of 3°C/min and a frequency of 1 Hz.

The creep and recovery behavior of the polymers was evaluated using a Perkin–Elmer thermomechanical analyzer Pyris TMA-7 in a three-point bending mode with a constant span of 10 mm. The samples were placed onto the bottom support and the top probe was adjusted to just contact the sample. The oven was set to the desired temperature and the sample was allowed to equilibrate for 10 min. Subsequently, a contact pressure of 100 Pa was placed on

Table 2
Structure and physical properties of the native and conjugated fish oil polymers

Sample	Density (kg/m^3)	T_g (°C)	Structure (wt%)		
			Crosslinked	Free oil	Oil incorporated
FO-DVB-38	1000	66	74.1	23.5	39.0
FO-DVB-NBD-38	1012	79	72.5	27.3	37.7
FO-DVB-DCP-38	1015	–	67.6	32.1	30.3
CFO-DVB-38	1005	11	83.1	16.5	46.0
CFO-DVB-NBD-38	1024	108	83.5	15.0	50.0
CFO-DVB-DCP-38	1020	113	83.1	15.9	46.5

the sample. The creep experiments were initiated by applying stresses of 0.03, 0.07, or 0.20 MPa, respectively and the resulting strain was recorded for 60 min. At applied stresses greater than 0.20 MPa, the creep behavior is similar to the case of the 0.20 MPa (see Section 3), which is beyond the linear viscoelastic region. Thus, experiments with higher loading stresses were not included in this study. The stress was then released and the subsequent strain recovery process was monitored. For multi-cycle measurements, all the specimens were subjected to at least four cycles of loading and unloading histories. The above experiments were conducted in a dry nitrogen atmosphere.

3. Results

3.1. Dynamic mechanical properties

The temperature dependence of storage modulus E' and loss factor *tan* δ for the FO polymers is shown in Fig. 2a. The figure shows that the storage modulus of the plastics at room temperature is approximately 8×10^8 Pa. Expectedly, the modulus gradually decreases with increasing temperature until an elastic plateau appears at temperatures above 150°C. The elastic plateau indicates the existence of a stable crosslinked network in the bulk polymer. Typically, a broad glass transition was observed with the *tan* δ peak centered around 80°C. The broad transition region results from the extensive motion of chain segments diversified by crosslinking in these polymeric systems. Fig. 2b shows the corresponding DMA results for the CFO polymers. The glass transition temperature of these CFO polymers is approximately 110°C, and the room temperature modulus is greater than 1×10^9 Pa. These values are significantly higher than those of the FO polymers shown in Fig. 2a. The differences in the dynamic mechanical properties of the FO and CFO polymers are mainly due to the variations in the structures of the different polymers discussed later. The reactivity of carbon–carbon double bonds in the FO molecule significantly increases upon conjugation [9,10]. This high reactivity results in more oil molecules participating in the reactions and being incorporated into the crosslinking polymers when CFO is used in the original composition. As Table 2 shows, the amount of incorporated oil in the CFO polymers increased by almost 10 wt%, implying the presence of less unreacted free oil molecules in the CFO polymers. This hypothesis is supported by the increased moduli and glass transition temperatures observed for these polymers (see Fig. 2a and b).

3.2. Creep and recovery behavior and analysis

Fig. 3a and b shows the creep and subsequent strain recovery curves of the FO and CFO polymer specimens (i.e. FO-DVB-38, CFO-DVB-38) obtained from three stress levels at room temperature using a new sample for each testing condition. After 60 min of creep loading, the specimens were unloaded instantaneously to study the strain recovery behavior. The creep curves were found to have the same general form showing an instantaneous elastic strain on loading that is followed by a period of slow linear deformation. These two regions are separated by a transition zone that is more pronounced at high load level. As expected, high loading stress resulted in large creep strain. However, the final creep strain after 60 min of static loading was less than 0.5%, regardless of the applied stress level used. Another feature that is noteworthy in this study is that the CFO polymer showed larger creep strains than that of the FO polymer at the same load levels.

The recovery curves of the polymers typically show an instantaneous contraction by an amount equal to the initial elastic strain, followed by a period of slow recovery, which continues for 120 min after unloading. These two regions are separated by a transition region. After recovery for an additional 120 min, the observed residual strains show no further changes, and can therefore be considered to represent permanent deformation in the material. Large creep strain in the creep process results in higher residual strain in the subsequent recovery.

The time dependencies of the relaxed moduli in the creep and subsequent recovery processes at different loading levels are shown in Table 3. For convenience, the modulus at 10 s, E_{10}, was selected to represent the original modulus in the creep process. The table shows that the FO polymer has a higher creep modulus (lower creep compliance) than the CFO polymer over the time scale at the same load levels. This is inconsistent with the previous DMA results (the DMA data show that the CFO polymers have a higher

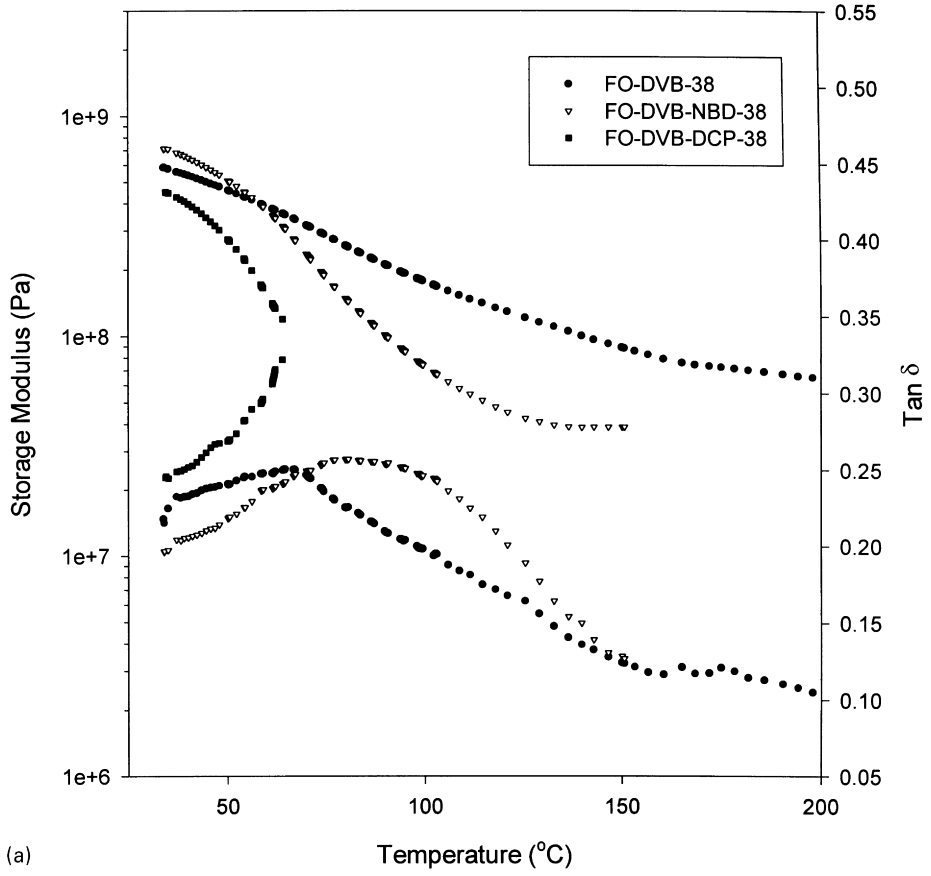

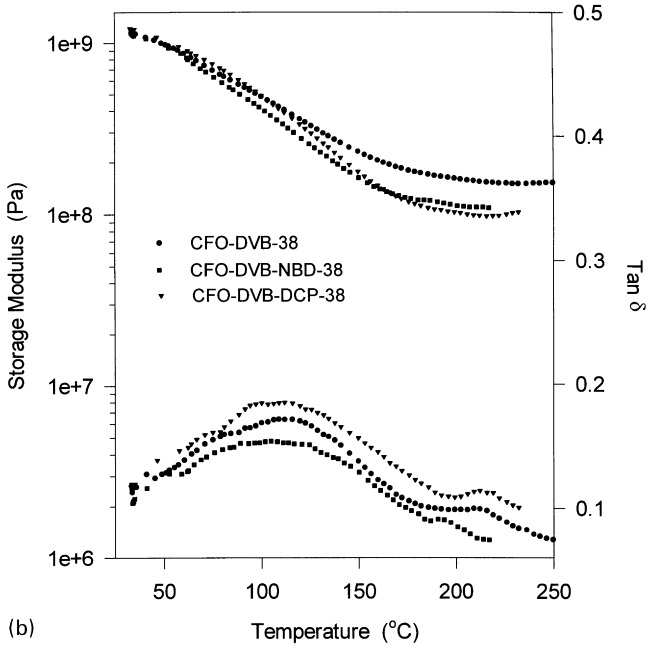

Fig. 2. Temperature dependence of storage modulus E' and loss factor *tan* δ for: (a) the native fish oil; and (b) the conjugated fish oil polymer specimens.

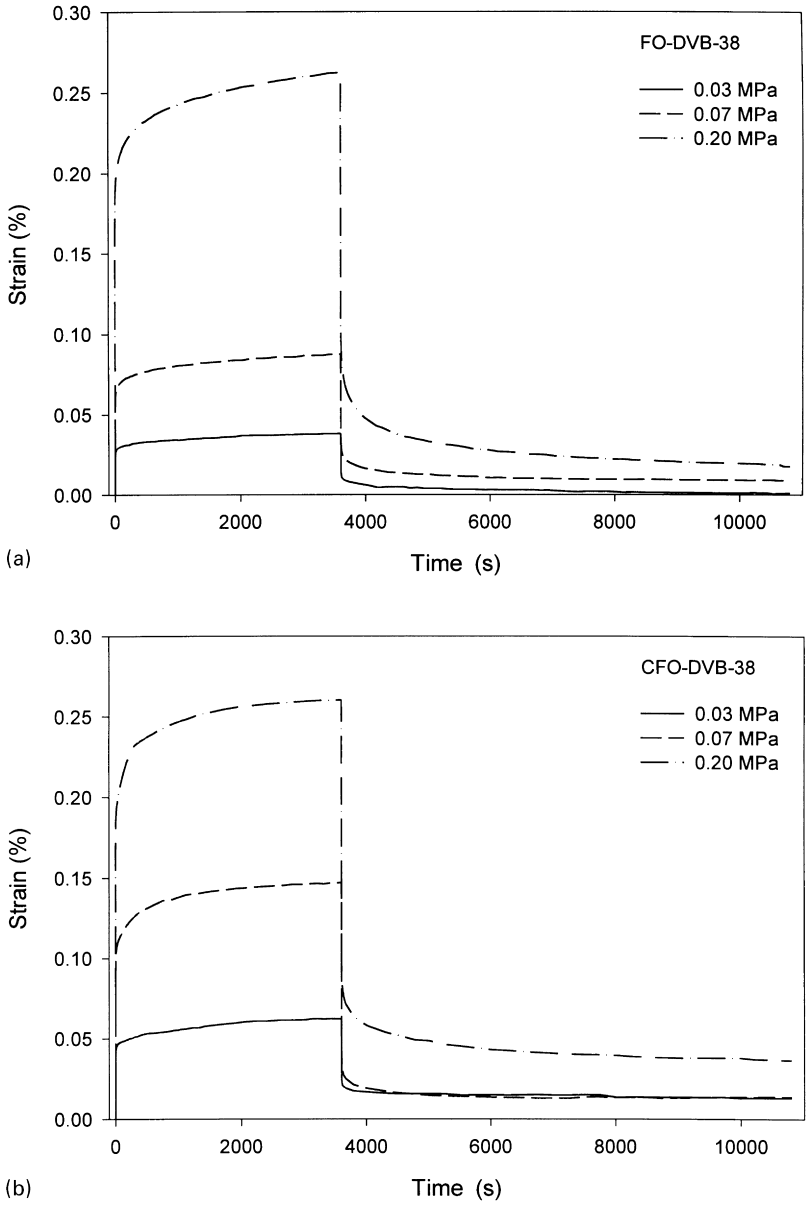

Fig. 3. Creep/recovery curves of: (a) the native fish oil polymer specimen FO-DVB-38; and (b) the conjugated fish oil polymer specimen CFO-DVB-38 with various load levels at room temperature.

storage modulus than the FO polymers). Repeated measurements confirm the reliability of the above DMA and creep data. To evaluate the creep resistance ability of the polymers, the modulus ratio $\Delta E_t/E_{10}$ in the creep process is defined as:

$$\frac{\Delta E_t}{E_{10}} = \frac{E_{10} - E_t}{E_{10}} \times 100\% \quad (1)$$

where E_t corresponds to the creep modulus at time t seconds. This ratio $\Delta E_t/E_{10}$ represents the percentage decrease in the original E_{10} after a time period t. Similarly, the modulus ratio $\Delta E'_t/E'_{10}$ in the recovery process is defined as:

$$\frac{\Delta E'_t}{E'_{10}} = \frac{E'_t - E'_{10}}{E'_{10}} \times 100\% \quad (2)$$

where E'_{10} is the initial modulus in the subsequent strain recovery process at 10 s after 3600 s of creep, and E'_t represents the modulus at the time t in the recovery process. The ratio $\Delta E'_t/E'_{10}$ thus corresponds to the percentage of the recovered modulus over the final creep modulus at the time t. The results in Table 3 show that both the FO and CFO polymer specimens have similar $\Delta E_{1000}/E_{10}$ and $\Delta E_{3600}/E_{10}$ values, implying that the modulus decreases in approximately

Table 3
Time dependent of the relaxed modulus in the creep and subsequent recovery processes at different loading levels

Sample	Load (MPa)	Modulus in creep process (Pa)					Modulus in recovery process (Pa)				
		E_{10}	E_{1000}	E_{3600}	$\Delta E_{1000}/E_{10}$ (%)	$\Delta E_{3600}/E_{10}$ (%)	E'_{10}	E'_{3600}	E'_{7200}	$\Delta E'_{3600}/E'_{10}$ (%)	$\Delta E'_{7200}/E'_{10}$ (%)
FO-DVB-38	0.03	1.68×10^9	1.33×10^9	1.19×10^9	21	29	3.55×10^8	8.10×10^8	1.07×10^9	128	201
	0.07	1.65×10^9	1.28×10^9	1.18×10^9	22	29	1.46×10^8	4.32×10^8	4.57×10^8	196	213
	0.20	1.11×10^9	8.59×10^8	7.94×10^8	22	29	4.56×10^7	1.81×10^8	4.32×10^8	297	847
CFO-DVB-38	0.03	1.06×10^9	8.43×10^8	7.49×10^8	21	30	2.29×10^8	2.86×10^8	3.21×10^8	25	40
	0.07	1.01×10^9	7.55×10^8	7.08×10^8	25	30	1.75×10^8	3.25×10^8	3.30×10^8	86	88
	0.20	1.11×10^9	8.41×10^8	7.98×10^8	24	28	5.98×10^7	1.05×10^8	1.14×10^8	76	91

the same manner in the observed creep process. However, in the subsequent recovery process, the $\Delta E'_t/E'_{10}$ values of the FO polymers are much higher than those of the CFO polymers. This observation further supports our earlier assertion that the FO polymer specimen has better creep and recovery properties than that exhibited by the CFO polymer.

For the most general case of a linear viscoelastic solid, the total creep strain ε_T is given by the Burgers Model, which is a series combination of the Maxwell and Kelvin–Voigt models [13,16]:

$$\varepsilon_T = \varepsilon_1 + \varepsilon_2 + \varepsilon_3 = \frac{\sigma}{E_1} + \frac{\sigma}{E_2}\left[1 - \exp\left(-\frac{E_2 t}{\eta_2}\right)\right] + \frac{\sigma t}{\eta_3} \quad (3)$$

Here ε_1 is the instantaneous elastic deformation; ε_2 is the delayed elastic deformation; and ε_3 is the Newtonian flow, which is identical to the deformation of a viscous liquid obeying Newton's law of viscosity. E_1 and E_2 are elastic moduli, η_2 and η_3 are viscosities, σ is the applied stress, and t is the creep time. In the linear viscoelastic range, the magnitudes of ε_1, ε_2 and ε_3 are exactly proportional to the magnitude of the applied stress, so that a creep compliance J_t can be defined, which is a function of time only:

$$J_t = J_1 + J_2 + J_3 = \frac{1}{E_1} + \frac{1}{E_2}\left[1 - \exp\left(-\frac{t}{\tau}\right)\right] + \frac{t}{\eta_3} \quad (4)$$

where J_1, J_2 and J_3 correspond to ε_1, ε_2 and ε_3, respectively, and the retardation time $\tau = \eta_2/E_2$. Generally, linear amorphous polymers show a significant J_3 (or ε_3) above their glass transition temperatures, when creep may continue until the specimen ruptures. But at lower temperatures J_1 and J_2 (or ε_1, ε_2) dominate. By comparison, crosslinked polymers do not show a J_3 (or ε_3) term, implying that recovery strain will return to zero at equilibrium.

In Eq. (4), a single retardation time is not sufficient to give an accurate description of the calculated viscoelastic compliance J_2. Therefore, the function can be modified according to the following equation [17,18]:

$$J_t = J_1 + J_2 + J_3 = \frac{1}{E_1} + \frac{1}{E_2}\left[1 - \exp\left(-\frac{t}{\tau_m}\right)^b\right] + \frac{t}{\eta_3} \quad (5)$$

where τ_m is the mean retardation time in the Guassian retardation spectrum [17], b is the Kohlrasch coefficient and can take values between 0 and 1. Fig. 4a and b give the temperature dependence of the creep compliances for the specimens FO-DVB-38 and CFO-DVB-38 at different loading levels. The observed creep compliance curves of the FO polymer specimen (see Fig. 4a) overlap with each other at the low loading levels of 0.03 and 0.07 MPa. But when the loading is 0.2 MPa, the creep compliance diverges significantly from the previous two curves. For the CFO polymer specimen (Fig. 4b), the difference in creep compliance at the various loading levels is negligible, especially

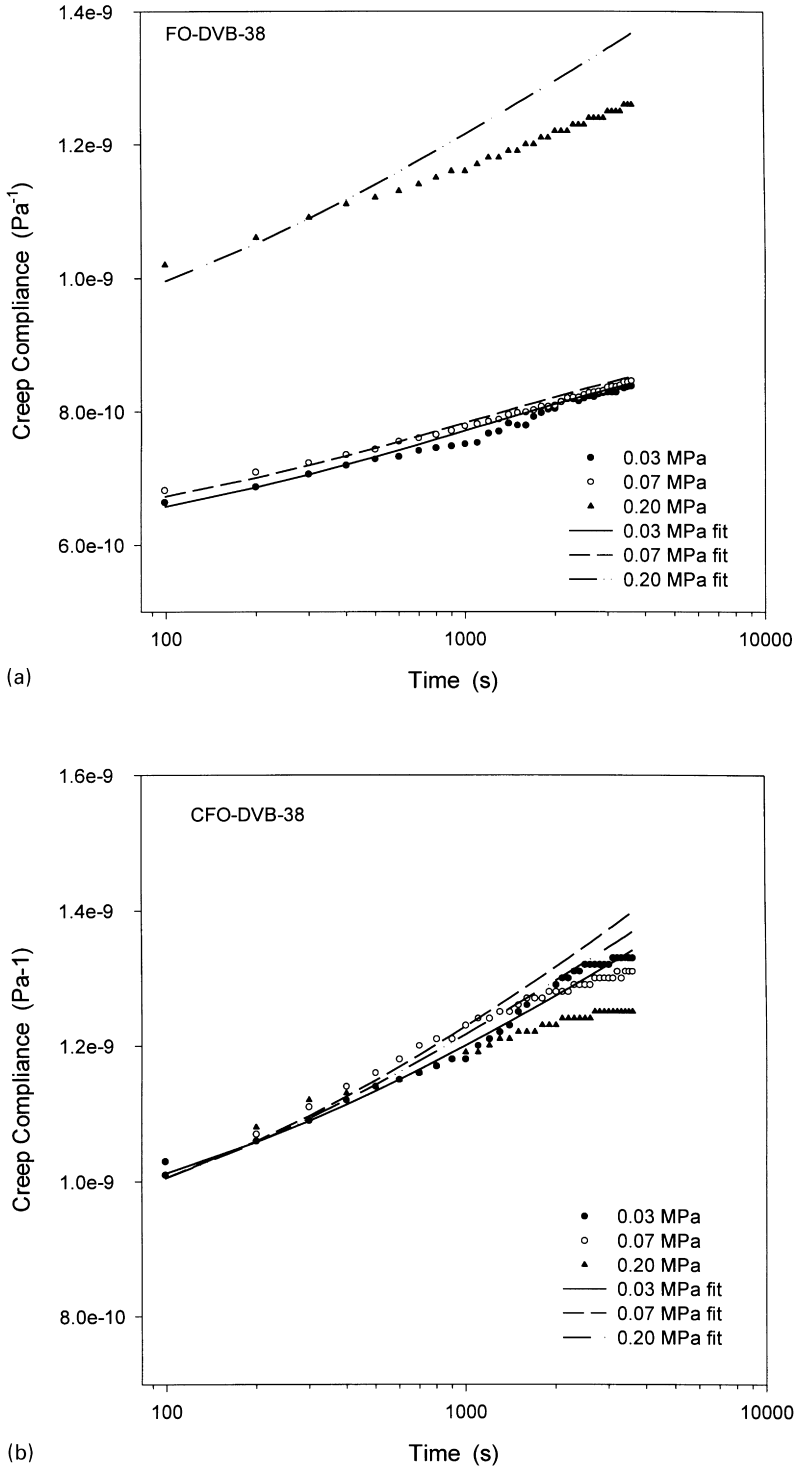

Fig. 4. Experimental creep compliance and model fitting of: (a) the native fish oil specimen FO-DVB-38; and (b) the conjugated fish oil specimen CFO-DVB-38 with various load levels at room temperature.

for the two low loading levels of 0.03 and 0.07 MPa. It seems that the creep compliance is independent of the stress at the two low levels. So, based on Eq. (4), the creep behavior of these oil-based polymer materials is in the linear viscoelastic range within the loading levels of approximately 0.03–0.07 MPa. Fig. 4a and b also give the model fitting results given by Eq. (5), which is based on linear viscoelastic theory. Table 4 lists the corresponding creep parameters obtained from the experimental data. In the linear viscoelastic range, the model fittings agree well

Table 4
Creep parameters for the polymeric materials

Samples	Loading (MPa)	Temperature (°C)	$1/E_1$ (Pa^{-1})	$1/E_2$ (Pa^{-1})	η_3 (Pa s)	τ_m (s)	b
FO-DVB-38	0.03	30	5.6×10^{-10}	3.5×10^{-10}	9.5×10^{13}	1200	0.45
	0.07	30	5.8×10^{-10}	3.3×10^{-10}	9.0×10^{13}	1100	0.45
	0.20	30	8.0×10^{-10}	6.0×10^{-9}	7.0×10^{13}	800	0.45
CFO-DVB-38	0.03	30	8.6×10^{-10}	5.5×10^{-10}	9.0×10^{13}	1300	0.45
	0.07	30	8.2×10^{-10}	6.5×10^{-10}	7.0×10^{13}	1200	0.45
	0.20	30	8.4×10^{-10}	6.0×10^{-10}	7.0×10^{13}	1000	0.45
FO-DVB-38	0.03	100	2.4×10^{-9}	1.5×10^{-9}	3.5×10^{12}	900	0.46
	0.03	150	8.5×10^{-9}	6.0×10^{-9}	2.4×10^{11}	700	0.49
CFO-DVB-NBD-38	0.03	100	2.8×10^{-9}	9.3×10^{-10}	8.0×10^{12}	1100	0.46
	0.03	150	4.0×10^{-9}	1.9×10^{-9}	4.0×10^{11}	800	0.49
CFO-DVB-NBD-38	0.03	30	7.5×10^{-10}	2.8×10^{-10}	2.0×10^{13}	1300	0.45
	0.03	100	2.7×10^{-9}	2.5×10^{-9}	2.8×10^{12}	1100	0.46
	0.03	150	5.8×10^{-9}	4.3×10^{-9}	2.8×10^{11}	800	0.49
CFO-DVB-DCP-38	0.03	30	7.7×10^{-10}	4.0×10^{-10}	2.0×10^{13}	1300	0.45
	0.03	100	2.5×10^{-9}	1.8×10^{-9}	3.5×10^{12}	1100	0.46
	0.03	150	6.8×10^{-9}	5.7×10^{-9}	1.4×10^{11}	800	0.49

with the experimental results. However, at high loading level, the poor agreement between the experimental and theoretical results is quite obvious, especially for the FO polymer specimens.

To determine the effect of temperature on the creep behavior of the polymers, we performed the creep experiments on the specimens at different temperatures at a loading level of 0.03 MPa within the linear viscoelastic range. Fig. 5a and b give the compliance results of the FO and CFO polymer specimens at 30, 100 and 150°C. Both figures show a strong dependence of the creep compliance on the temperature. At higher temperatures, the change in the creep compliance becomes pronounced as a result of the decrease in relaxation time (relaxation spectrum moves downwards). The model fits (lines) to the experimental data according to Eq. (5) are also shown in the figures (the creep parameters are summarized in Table 4). In all cases, there is very little difference between the model fits and the data. The creep model provides a reliable prediction of the creep behavior of both FO and CFO polymers over a wide range of temperatures in the linear viscoelastic region.

Table 5 gives the creep results of the polymer specimens with different comonomers. For the CFO polymers, little difference in $\Delta E_{100}/E_{10}$ and $\Delta E_{300}/E_{10}$ was obtained after the second comonomer was added. But, the results of the FO polymers were found to be dependent on the types of comonomer used. Generally, the polymer specimens with DVB as the comonomer show good creep resistance properties. The results show that the creep behavior of the polymer specimens based on different comonomers is also well fitted by Burger's model.

3.3. Multiple cycle creep and recovery behavior

Fig. 6a and b shows the multiple cycle creep and recovery behavior of the FO and CFO polymer specimens. The specimens show good creep resistance properties at room temperature. At high temperatures, however, the creep strains increase sharply due to the increased mobility of the molecules. It was observed that the strain increased as the number of creep and recovery cycles was increased. This result may be interpreted by the values of the time constant for recovery, which is much smaller than that for the creep process. Thus, the time for strains to relax is much longer than the time required for the strains to develop during creep. This effect is greater than that predicted by linear viscoelastic theory and is exacerbated by the possible buildup of plastic strains and/or other permanent microstructural changes.

The recovery for each creep and recovery cycle was calculated from the following equation:

$$R(n) = \frac{\varepsilon_{300(2n-1)} - \varepsilon_{600n}}{\varepsilon_{300(2n-1)} - \varepsilon_{600(n-1)}} \times 100\% \quad (6)$$

where $R(n)$ is the recovery of the creep strain in the nth creep and recovery cycle; ε_x is the strain at the time x seconds. Fig. 7a and b gives the results of the calculated $R(n)$ values. The figures show that recovery $R(n)$ increases with the number of cycles. At low temperature, the recovery is high. But at high temperature, the recovery becomes lower. In comparison with the polymer FO-DVB-38, the CFO-DVB-38 specimen shows higher recovery in each creep and recovery cycle.

4. Discussion

Both the FO and CFO can be used to produce hard and stiff polymers having moduli comparable to those of conventional plastics. The DMA measurements show that the CFO polymers have higher moduli and glass transition temperatures. Therefore, the CFO polymers should be more creep-resistant than the FO polymers. However, the creep and recovery measurements indicate that the FO polymers

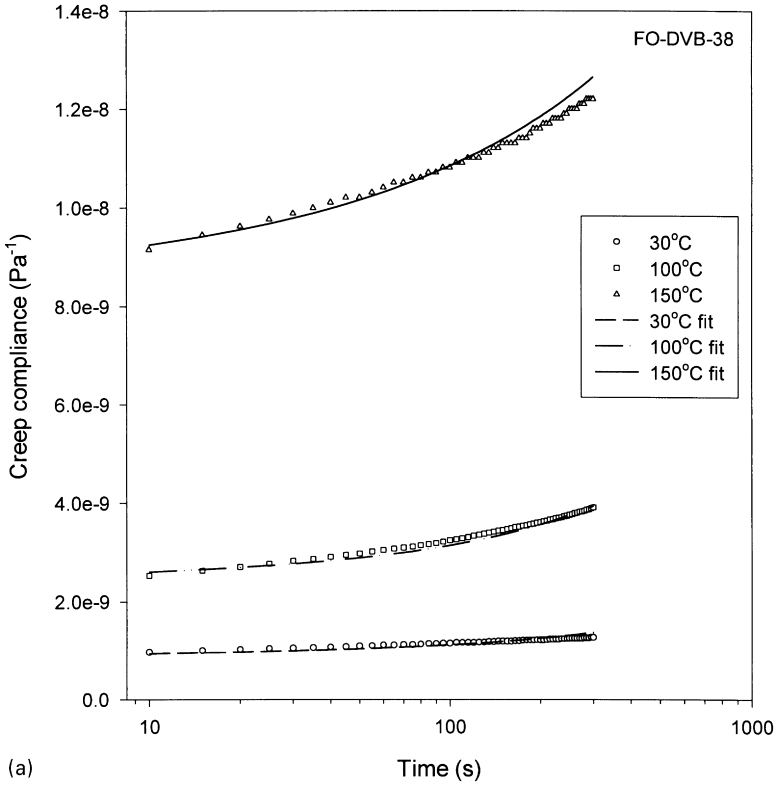

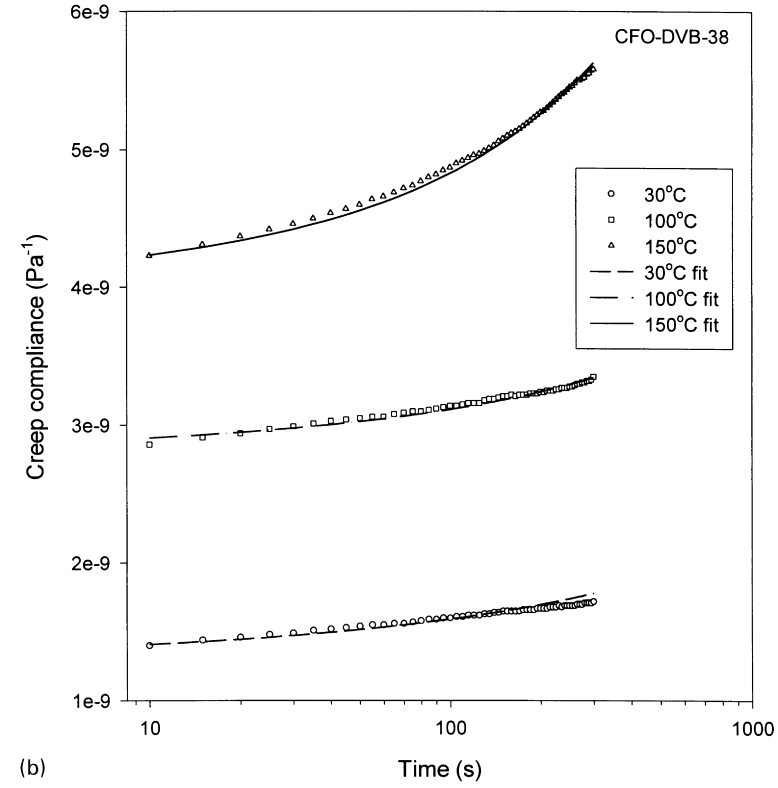

Fig. 5. Experimental creep compliance and model fitting of the specimens: (a) FO-DVB-38; and (b) CFO-DVB-38 at different temperatures.

Table 5
Relaxed creep modulus for the polymeric materials at room temperature

Sample	Creep modulus (Pa)				
	E_{10}	E_{100}	E_{300}	$\Delta E_{100}/E_{10}$ (%)	$\Delta E_{300}/E_{10}$ (%)
FO-DVB-38	1.62×10^{9}	1.40×10^{9}	1.32×10^{9}	16	21
FO-DVB-NBD-38	1.01×10^{9}	7.70×10^{8}	7.01×10^{8}	23	30
FO-DVB-DCP-38	5.05×10^{8}	2.84×10^{8}	2.25×10^{8}	44	56
CFO-DVB-38	1.06×10^{9}	8.98×10^{8}	8.55×10^{8}	15	19
CFO-DVB-NBD-38	1.32×10^{9}	1.11×10^{9}	1.02×10^{9}	15	23
CFO-DVB-DCP-38	1.21×10^{9}	1.01×10^{9}	9.62×10^{8}	17	20

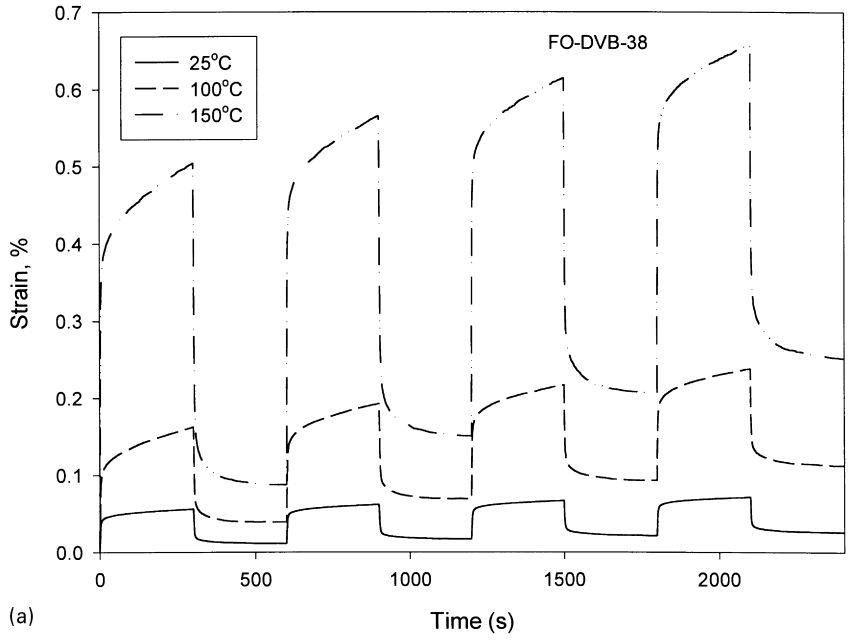

(a)

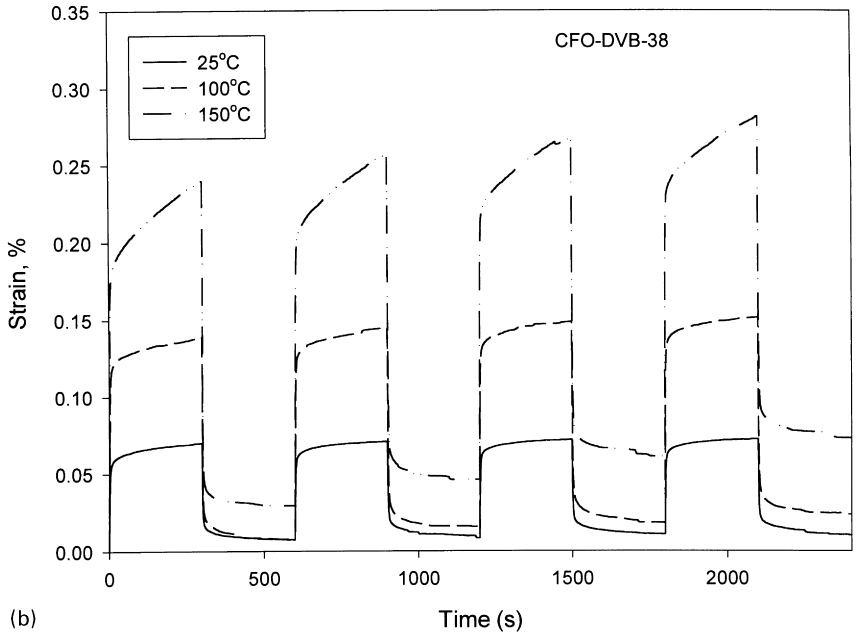

(b)

Fig. 6. Multi-cycle creep/recovery behaviors of the specimens: (a) FO-DVB-38; and (b) CFO-DVB-38 at different temperatures.

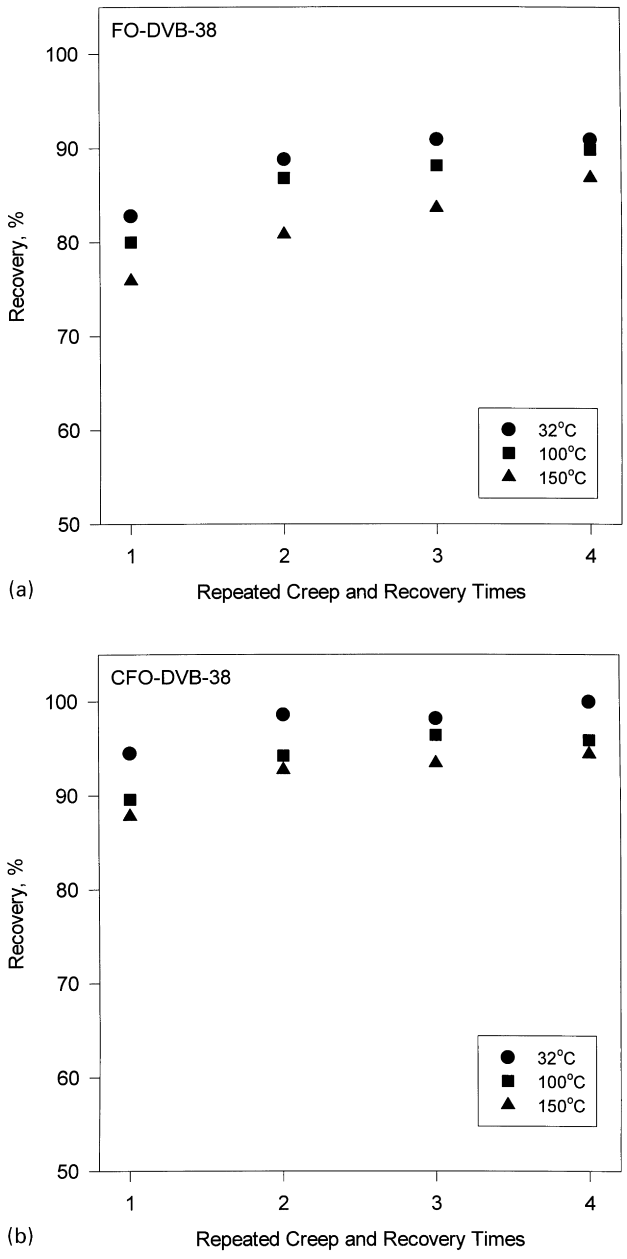

Fig. 7. The dependence of the recovery on the cycle times for the specimens: (a) FO-DVB-38; and (b) CFO-DVB-38 at various temperatures.

have relatively good creep properties (lower creep strains). The residual strains after recovery are also lower, with the specimen FO-DVB-38 showing almost full recovery after the removal of a creep load of 0.03 MPa (see Fig. 3a). To elucidate this contradictory result, it is necessary to analyze the structures of these thermosetting polymers.

The materials of this study have been shown to be thermosetting polymers with high crosslinking densities as reported elsewhere [8,14]. Generally, 15–30 wt% soluble substances have been obtained from the polymers after Soxhlet extraction by methylene chloride (see Table 2). These soluble substances are unreacted free oils at ambient temperature. Most of the bulk polymer, however, is composed of the insoluble substances (65–80 wt%) (Table 2). These insoluble substances are crosslinked molecules resulting from cationic copolymerization facilitated by the multitude of double bonds in both the fish oil molecules and the comonomers used. The insoluble substances are highly crosslinked molecules, which cannot be swollen by good solvents, such as methylene chloride, THF, etc. These results suggest that the structure of the bulk polymer is that of a *highly crosslinked* structure plasticized by a certain amount of unreacted free oil. Despite the high yield of insoluble substances, they exist in the form of distinct flakes, instead of a whole block, after Soxhlet extraction (see Fig. 8a and b). The average diameter of the crosslinked substances obtained after extraction of the FO polymers is approximately 5.0 mm, while that of the materials from the CFO polymers is much smaller, ca. 2–3 mm, which are ascribed to the reaction mechanisms given elsewhere [12]. In other words, the crosslinked portion in the bulk polymer is not an ideal giant molecule, but many discrete giant molecules linked together with *lightly crosslinked* molecules along their interfaces as depicted in Fig. 9. These interfaces are sufficiently weak to be destroyed by the solvent CH_2Cl_2 used in the Soxhlet extraction process.

In general, full recovery of the crosslinked polymers is expected at low creep strains [13,16]. In this study, the loading level used was between 0.03 and 0.20 MPa, and the creep strain observed was less than 0.30%. However, almost all the measurements showed the presence of irreversible strains (see Fig. 3a and b). These irreversible strains become pronounced when high loading is employed. The observed residual strains are ascribed to the non-identical crosslinking structure obtained from the various oils and comonomers used and to the existence of unreacted free oil molecules in the bulk polymer. Fig. 9 suggests that the *highly crosslinked* molecules make up the matrix of the bulk polymer. These *highly crosslinked* substances themselves do not produce any irreversible strains after creep and recovery processes. However, the interfaces between these substances are composed of many *lightly crosslinked* molecules. These molecules at the interfaces are easier to deform upon loading than the *highly crosslinked* molecules at room temperature. The existence of the free oil molecules in the bulk polymer, which prefer to reside in the interfaces, facilitates movements of the interfacial molecules under loading. When the stress is removed, these *lightly crosslinked* molecules tend to recover to their original state. The driving force for this is the stored elastic energy in the creep process. Due to their viscoelastic nature, these molecules cannot completely return to their original state like the perfectly crosslinked molecules, and as a result various amounts of irreversible strains are obtained. In fact, these irreversible strains correspond to the displacement of the inter-distance among the *highly crosslinked* substances, which constitute the bulk of the thermosetting polymers.

The DMA results show that the CFO polymers have higher storage moduli and glass transition temperatures

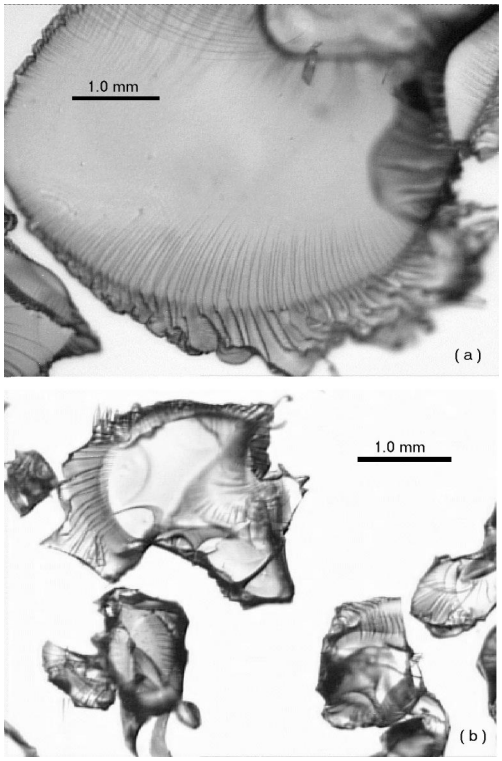

Fig. 8. Optical microscope photographs of the insoluble substances from the samples: (a) FO-DVB-38; and (b) CFO-DVB-38 remaining after extraction by methylene chloride.

than the FO polymers. This observation is due primarily to the presence of less unreacted free oil molecules in the bulk CFO polymers relative to the amount present in the FO polymers. In the creep measurements shown in Fig. 3a and b, the FO polymer specimen shows better creep resistance than the CFO polymer at room temperature. This observation is confirmed by the creep strains under the same conditions (Fig. 3a and b), and the results of the creep moduli listed in Table 3. The reason for this observed discrepancy is not clear. One plausible explanation may be due to the complex interaction between the *lightly crosslinked* molecules at the interfaces and the ones from the *highly crosslinked* substances of the bulk polymer. As shown in Fig. 9, the actual differences between the *highly crosslinked* portions of the FO and CFO polymers is negligible. However, the size of the *highly crosslinked* portions of the CFO polymers is much smaller, so, the specific interfacial areas in the CFO polymer are likely to be significantly larger than those of the FO polymers. A large interfacial area is undesirable for enhanced mechanical properties of the CFO polymers. As mentioned earlier, unreacted free oils exist in the bulk of the FO polymers. These free oils may function as plasticizers, and therefore decrease the moduli and glass transition temperatures of the FO polymers.

The discrepancy in the results of this study may also be ascribed to differences in the deformation modes used in the creep and DMA measurements. For example, in the creep

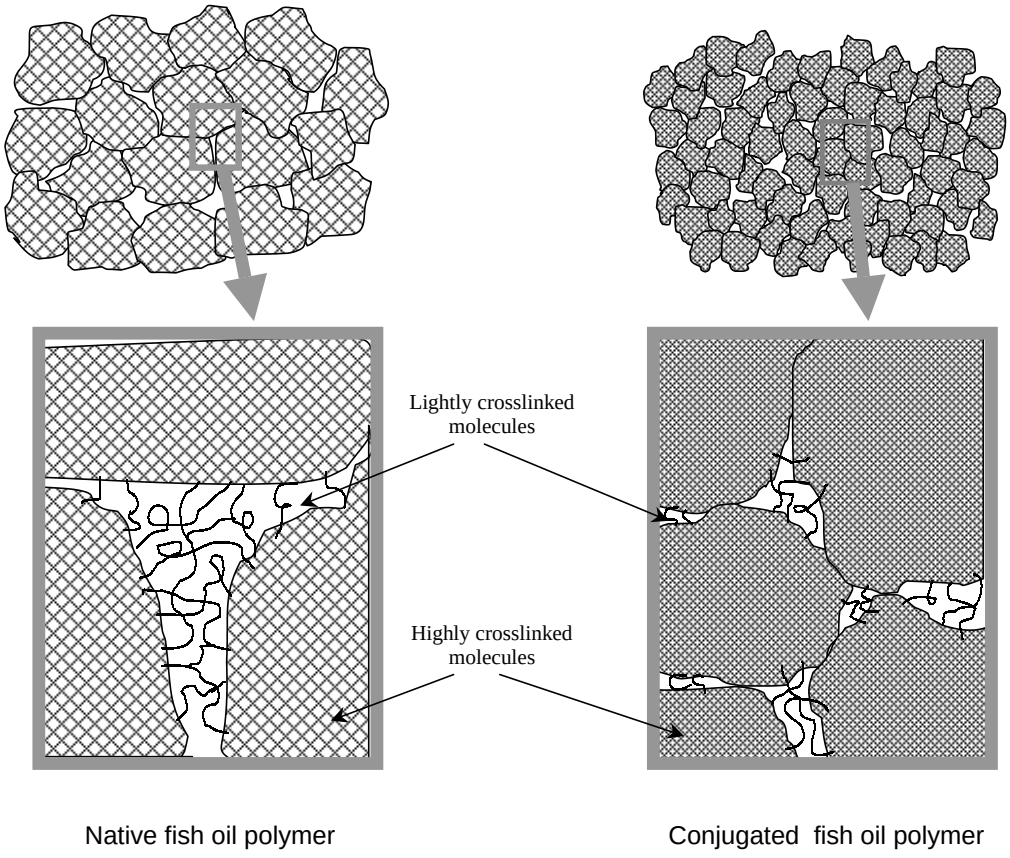

Fig. 9. Schematic representation of the microstructures of the native and conjugated fish oil thermosetting polymers.

measurements at room temperature, the applied stress is static. Although both of the *highly* and *lightly crosslinked* portions of these polymers will respond to stress, the *lightly crosslinked* molecules at the interfaces are expected to respond more than the *highly crosslinked* molecules to the static deformation. If we compare the FO and CFO samples, the creep behavior is predominantly affected by the large difference in the interfaces. The effect of the free oil in the polymer bulk is negligible in this case. The large difference in the interfacial areas between FO and CFO polymers may be the reason why the CFO polymer shows relatively high creep strains at the same loading levels. By comparison, the applied stress is dynamic in the dynamic mechanical analysis. According to WLF theory [19], decreasing time or increasing frequency is equivalent to increasing temperature. In DMA measurements, the *highly crosslinked* substances become more mobile than in the creep measurements. Therefore, both the *highly crosslinked* and *lightly crosslinked* molecules cooperatively respond to the loading stress. The effect of the interfaces therefore decreases, and the effect of the free oil present in the bulk polymer may become dominant. The observed modulus should be the average contributions from the cooperative deformation of the two types of molecules just mentioned. The CFO polymers show higher moduli and glass transition temperatures from the dynamic mechanical analysis.

The validity of the above discussion is consistent with the results of the creep measurements performed at various temperatures. At room temperature, the CFO polymer shows higher creep compliance than the FO polymer. But, the FO polymer has higher creep compliances at elevated temperatures than that CFO polymer (see Fig. 5a and b). As discussed above, the effect of the interfaces is dominant at room temperature. At higher temperatures (equivalent to increasing frequencies from WLF theory), the mobility of both *highly crosslinked* and *lightly crosslinked* molecules increase, and the effect of the interfaces diminishes, while the effect of the free oil in the bulk polymer becomes dominant.

In the multi-cycle creep and recovery measurements, the creep and recovery time was ten minutes for each creep and recovery cycle. The *lightly crosslinked* molecules at the interfaces are expected to play a dominant role in these measurements. The creep strain may not be enough to break up the *lightly crosslinked* molecular structure in the FO and CFO polymer specimens. But, in the FO polymer, more free oil present mostly in the *lightly crosslinked* regions facilitates displacement of some polymer molecules under the test conditions. The recovery $R(n)$ observed for both the FO and CFO polymer specimens appears to be consistent with the deformation mechanism discussed above.

In this study, the creep strains are less than 0.3%, well below 1%, which is generally the upper limit for polymers to show linear viscoelastic behavior. But, when 0.20 MPa is applied to these oil-based polymers, the results show non-linear viscoelastic behavior even at a creep strain of 0.25% (see Fig. 3a and b). This result cannot be easily explained by the structure of the polymers themselves. The reason may probably be due to the limitation of the TMA technique itself. In this work, three-point bending mode was used. When certain values of creep strain are achieved, the deformation of the specimen would probably not be the pure tensile opening mode (*Mode-I*) [20].

5. Conclusion

Thermosetting polymers have been produced by the cationic copolymerization of FO or CFO with a number of diene comonomers using boron trifluoride diethyl etherate as an initiator. The resulting polymers have glass transition temperatures ranging from 80 to 120°C, and storage moduli of about 1.0×10^9 Pa at room temperature. The creep and recovery behavior of the FO and CFO polymers is similar to each other in general form. The compliance can be well fitted by the Burger model for a linear viscoelastic solid within the loading levels of 0.03–0.07 MPa at room temperature, or at 0.03 MPa over a wide temperature range. Generally, the CFO polymer shows relatively low creep-resistance properties at room temperature. But, at temperatures above their glass transition temperatures (80–120°C), the creep properties of the CFO polymers are much better than those of the FO polymer, which is consistent with the dynamic mechanical analysis results. The differences in the above measurements are well explained on the basis of WLF theory and the relatively complex structures of these thermosetting polymers. It would appear that these materials can be chemically tailored to meet specific applications requiring environmentally benign biodegradation after service.

Acknowledgements

This project was supported by the Iowa Soybean Promotion Board.

References

[1] Bisio AL, Xanthos M. How to manage plastics waste: technology and market opportunities, New York: Hanser, 1995.
[2] Mustafa N. Plastics waste management: disposal, recycling and reuses, New York: Marcel Dekker, 1993.
[3] Kramer O. Biological and synthetic polymer networks, New York: Elsevier, 1988.
[4] Ackman RG. In: Barlow SM, Stansby ME, editors. Nutritional evaluation of long-chain fatty acids in fish oil, New York: Academic Press, 1982.
[5] Gruger EH. In: Stansby ME, editor. Fish oils: their chemistry, technology, stability, nutritional properties and uses, Connecticut: AVI Publishing Company, 1967.
[6] Stansby ME, Schlenk H, Gruger EH. In: Stansby ME, editor. Fish oils in nutrition, New York: Van Nostrand Reinhold, 1990.

[7] Technology International Exchange, Inc. Certificate of Analysis for Pronova Fish Oil, Pronova Biocare, 1996.
[8] Li F, Marks DW, Larock RC, Otaigbe JU. SPE ANTEC Tech Papers 1999;3:3821–5.
[9] Faust R, Shaffer TD. Cationic polymerization: fundamentals and applications, ACS Symposium Series. Washington, DC: ACS, 1997.
[10] Matyjaszewski K. Cationic polymerizations: mechanisms, synthesis and applications, New York: Marcel Dekker, 1996.
[11] Marc LG. Organic chemistry, Reading, MA: Addison-Wesley, 1984.
[12] Li F, et al. Unpublished results.
[13] Nielsen LE, Landel RF. Mechanical properties of polymers and composites, New York: Marcel Dekker, 1994.
[14] Li F, Marks DW, Larock RC, Otaigbe JU. Submitted for publication.
[15] Marks DW, Larock RC. In preparation.
[16] Ward IM, Hadley DW. An introduction to the mechanical properties of solid polymers, New York: Wiley, 1993.
[17] Markis C, Villontreix G. J Appl Polym Sci 1998;69:1983–91.
[18] Williams G, Watts DC. Trans Faraday Soc 1970;66:80.
[19] Ferry JD. Viscoelastic properties of polymers, New York: Wiley, 1961.
[20] Kinloch AJ, Young RJ. Fracture behavior of polymers, New York: Applied Science, 1983.